Metabolic Engineering 59 (2020) 36–43

Contents lists available at ScienceDirect

Metabolic Engineering

journal homepage: www.elsevier.com/locate/meteng

In vivo evolutionary engineering of riboswitch with high-threshold for N-acetylneuraminic acid production

Qingxiao Pang[a], Hao Han[a], Xiaoqin Liu[a], Zhiguo Wang[b], Quanfeng Liang[a], Jin Hou[a], Qingsheng Qi[a,c,**], Qian Wang[a,*]

[a] State Key Laboratory of Microbial Technology, National Glycoengineering Research Center Shandong University, Jinan, 250100, PR China
[b] Institute of Ageing Research, School of Medicine, Hangzhou Normal University, Hangzhou, 311121, PR China
[c] CAS Key Lab of Biobased Materials, Qingdao Institute of Bioenergy and Bioprocess Technology, Chinese Academy of Sciences, Qingdao, 266101, PR China

ARTICLE INFO

Keywords:
Riboswitch
Evolution *in vivo*
Threshold
Biosensor
N-acetylneuraminic acid

ABSTRACT

Riboswitches with desired properties, such as sensitivity, threshold, dynamic range, is important for its application. However, the property change of a natural riboswitch is difficult due to the lack of the understanding of aptamer ligand binding properties and a proper screening method for both rational and irrational design. In this study, an effective method to change the threshold of riboswitch was established *in vivo* based on growth coupled screening by combining both positive and negative selections. The feasibility of the method was verified by the model library. Using this method, an N-acetylneuraminic acid (NeuAc) riboswitch was evolved and modified riboswitches with high threshold and large dynamic range were obtained. Then, using a new NeuAc riboswitch, both ribosome binding sites and key gene in NeuAc biosynthesis pathway were optimized. The highest NeuAc production of 14.32 g/l that has been reported using glucose as sole carbon source was obtained.

1. Introduction

Riboswitches are RNA-based regulators of gene expression composed of a ligand-sensing aptamer domain followed by an overlapping expression platform (Barrick, 2009; Breaker, 2011). As an RNA regulatory element, they plays an important role in the regulation of metabolism *in vivo* (Sherwood and Henkin, 2016). The aptamers response to intracellular metabolite concentrations by altering conformation of allosterically bound ligand metabolites, leading to premature transcription termination, inhibition in translation initiation or mRNA degradation (Barrick et al., 2004; Corbino et al., 2005; Lee and Oh, 2015a; Nudler and Mironov, 2004; Roth and Breaker, 2009; Winkler and Breaker, 2005; Winkler et al., 2004). So far, many natural riboswitches have been excavated (McCown et al., 2017; Pavlova et al., 2019; Serganov and Nudler, 2013), mainly responding to fundamental metabolites including coenzymes, nucleobases or their derivatives, amino acids, and other small molecule ligands. As a riboswitch component, ribozymes cleave itself in a highly sequence-specific manner (de la Pena et al., 2017; Felletti and Hartig, 2017; Gebetsberger and Micura, 2017) to control gene expression (Auslander et al., 2010).

In synthetic biology, riboswitches were used as *in vivo* biosensors (Aghdam et al., 2016; Ogawa, 2011; Rogers et al., 2016; Williams et al., 2016; Zhang et al., 2015). Compared to protein-based biosensors, riboswitches based biosensors are usually specific to a limited number of metabolites, but faster response time and less metabolic burden on cells (Liu and Arkin, 2010). Furthermore, riboswitches can be combined as tandem copies, leading to a tighter regulation of gene expression (Henkin, 2008). Therefore, riboswitches have been extensively applied to substrate detection, dynamic regulation of cell metabolism and strains screening (Lee and Oh, 2015b; Mayer and Famulok, 2006; Penchovsky and Stoilova, 2013; Wang et al., 2015; Zhou and Zeng, 2015). New aptamers have also been designed and selected using an *in vitro* technology called SELEX (Systematic Evolution of Ligands by Exponential enrichment) (Carothers et al., 2009; Ellington and Szostak, 1990; Findeiss et al., 2017; Ogawa, 2011).

However, the properties of riboswitch, such as the threshold, sensitivity and response range (Mannan et al., 2017), do not meet practical metabolic applications, and the precise tuning them remains a significant challenge. Studies showed that RNA architecture influence threshold of riboswitch (Souliere et al., 2013). SELEX technology was reported to screen riboswitches with different performances, but need much time and labor (Jang et al., 2017). Introducing mutations in the

* Corresponding author.
** Corresponding author. State Key Laboratory of Microbial Technology, National Glycoengineering Research Center Shandong University, Jinan, 250100, PR China.
E-mail addresses: qiqingsheng@sdu.edu.cn (Q. Qi), qiqi20011983@sdu.edu.cn (Q. Wang).

https://doi.org/10.1016/j.ymben.2020.01.002
Received 21 October 2019; Received in revised form 26 November 2019; Accepted 4 January 2020
Available online 16 January 2020

ligand binding region was possible to change ligand binding capabilities (Serganov et al., 2008; Souliere et al., 2013).

Growth coupled screening methods have been developed for high throughput screening (Dietrich et al., 2010; Lee and Oh, 2015b) and population quality control (Xiao et al., 2016). A method based on *tetA*, coding tetracycline resistance protein, was effective to screen for appropriate riboswitch mutants. *TetA* is a bifunctional protein, which can transport nickel ions (Ni^{2+}) into cells to inhibit cell growth, and can excrete tetracycline from cells to obtain tetracycline resistance (Muranaka et al., 2009).

In this study, a strategy to evolve and screen the N-acetylneuraminic (NeuAc) riboswitches *in vivo* was established. Base-saturation mutations on binding loops changed the affinity of the riboswitch and affected threshold of riboswitch. Then a selected high threshold riboswitch was used to optimize pathway and evolve key enzymes. An engineered strain with the highest NeuAc titer was obtained using glucose as the sole carbon source.

2. Materials and methods

2.1. Bacterial strains, plasmids and media

Bacterial strains and plasmids used in this study are listed in Table S1. *Escherichia coli* DH5α were used for cloning purposes and were propagated in Luria-Bertani (LB) medium at 37 °C under aeration. For Ni^{2+} and tetracycline selection, M9B minimal medium was used. This medium contained (per liter): 6 g KH_2PO_4, 24 g K_2HPO_4, 1 g $Na_3Citrate{\cdot}2H_2O$, 10 g $(NH_4)_2SO_4$, 0.6 g $MgSO_4{\cdot}7H_2O$ and 0.025 g $CaCl_2{\cdot}2H_2O$. The trace elements were supplied as follows (per liter): 0.01 mg $CoCl_2{\cdot}6H_2O$, 0.01 mg H_3BO_3, 0.01 mg $CoSO_4{\cdot}5H_2O$, 0.5 mg $FeSO_4{\cdot}7H_2O$, 0.033 mg $MnSO_4{\cdot}H_2O$, 0.38 mg $ZnSO_4{\cdot}7H_2O$ and 0.01 mg $NaMoO_4{\cdot}2H_2O$. Vitamin B1 was added to a final concentration of 10 μg/ml. The strains DN5 were used for fermenting to produce NeuAc. Modified terrific broth (MTB) medium (12 g/l tryptone, 24 g/l yeast extract and 5 g/l NaCl) was used for NeuAc fermentation. Antibiotics were added when necessary (ampicillin 100 μg/ml, kanamycin 25 μg/ml, chloramphenicol 17 μg/ml and spectinomycin 100 μg/ml).

2.2. Plasmid construction

Oligonucleotides used in this work are listed in Table S2. A high-fidelity DNA polymerase (Takara, Japan) was used for plasmid construction purpose and 2 × Taq MasterMix (CWBIO, China) was used for colony PCR. Plasmid 99a-rs-tetA-gfp was constructed as follows. The *sfgfp* gene was generated by PCR with primers 99a-gfp-F and tetA-gfp-R, using psfGFP-ssrA as the template. To extend homology arm, resulting fragment was used as template to perform another cycle of PCR using primers 99a-gfp-F and tetA-gfp-R2, generating fragment gfp2. Plasmid 99a-rs-tetA digested with *Eco*RI was used as the backbone after gel purification. Then, *gfp2* and digested 99a-tetA were assembled together using an assembly method (Gibson, 2011; Gibson et al., 2009). The assembled plasmid was transformed into strain DH5α, and colony PCR and sequencing were performed to verify the correctness of the plasmid. For 99a-tetA-gfp construction, 99a-rs-tetA-gfp was digested with *Eco*RI and *Xba*I. The fragment was generated by PCR using primers XbaI-tetA-F and EcoRI-gfp-R, and then was digested with *Eco*RI and *Xba*I. Then, two fragments were ligated together using T4 DNA ligase for half an hour at 25 °C.

The riboswitch mutant library was constructed as follows. Eighteen primers are mixed in Table S3, the fragment rs-tetA-gfpm was generated by PCR with mixed primers and primer tetA-gfp-F. Plasmid 99a-rs-tetA-gfp was amplified by PCR using primers neuRS-F and 99a-R, and the fragment was used as the backbone after *Dpn*I digestion and PCR recycling. Then, rs-tetA-gfpm and the backbone were assembled together. Plasmid 99a-rsd-tetA was constructed by reverse PCR using primers rsd-F and rsd-R, and resulting fragment was then digested with *Dpn*I and assembled. For p15A-SdT construction, the riboswitch on p15A-S was mutated by reverse PCR using primers rsd-F and rsd-R and was transformed into *E. coli* DH5α after *Dpn*I digestion. For p15A-SdT construction, *sfgfp* was used to replace *tetA* by Gibson assembly.

The plasmid pBac was constructed by replacing the isozymes of Age and NeuB on pB. Gene $neuB_c$ (*neuB* gene from *Campylobacter jejuni*) was generated by PCR using primers cam-F and cam-R, and gene age_a (*age* gene from *Anabaena* sp. *CH1*) was generated by PCR using primers ana-F and ana-R. Plasmid pB was amplified by PCR using primers pB-F and pB-R, and the fragment was used as the backbone after *Dpn*I digestion and PCR recycling. Then, age_a, $neuB_c$ and the backbone were assembled together using Gibson assembly.

Plasmid pBac-based RBS library was generated as follows. The backbone was amplified from pBac using primers pBac-F1 and pBac-R1. The four genes with mixed RBS were amplified from pBac using mixed primers neuB-F1/neuB-F2/neuB-F3/neuB-F4/neuB-R, ana-F1/ana-F2/ana-F3/ana-F4/ana-R, GNA1-F1/GNA1-F2/GNA1-F3/GNA1-F4/GNA1-R and glmS-F1/glmS-F2/glmS-F3/glmS-F4/glmS-R, respectively. Then the five fragments were assembled together using the Gibson method. Positive rate of the library was detected by colony PCR using primers pB-testF/pB-testR.

The age_c mutant library was generated as follows. The backbone was amplified from pBac using primers pB-F/pBac-R2. Error-prone PCR was performed using Gene Morph II Random Mutagenesis kit (Agilent Technologies, USA) following the manufacturer's instructions. Randomly mutated age_c was amplified from pBac using primers ana-F2/ana-R and then were assembled together with the backbone using the Gibson method.

2.3. Strain cultivation

For NeuAc biosensor characterization using gfp as the reporter, a single colony was inoculated into 5 ml LB and incubated for 12 h at 37 °C and 220 rpm. 96-well plate was used to detect green fluorescence using a Multi-Detection Microplate Reader (Synergy HT, Biotek, USA) for 24 h cultivation by adding different amounts of NeuAc (0 g/l, 1 g/l, 2 g/l, 4 g/l, 8 g/l). For further characterization in shake flask, the preculture was inoculated into 50 ml of fresh M9B containing 20 g/l glucose with 2% inoculum. Different amounts of NeuAc (0 g/l, 4 g/l, 8 g/l) were added to the culture. Cultivation was maintained at 30 °C and 220 rpm. The fluorescence intensity was determined at 3 h intervals.

For optimizing the riboswitch screening method, a single colony was inoculated into 5 ml LB and cultivated for 12 h at 37 °C and 220 rpm. 96-well plate was used to detect green fluorescence using a Multi-Detection Microplate Reader for 24 h cultivation with different amounts of NeuAc (0 g/l, 1 g/l, 2 g/l, 4 g/l, 8 g/l) added to the culture. The preculture was then inoculated into 200 μl of fresh M9B minimal medium containing 20 g/l glucose and 200 μM Ni^{2+} with 1% inoculum. For further characterization in shake flasks, the preculture was then inoculated into 50 ml of fresh M9B minimal medium containing 20 g/l glucose and 200 μM Ni^{2+} with 1% inoculum. Different amounts of NeuAc (0–100 mM) were added to the culture at start. Cultivation was maintained at 30 °C and 220 rpm. Samples were taken at 4 h intervals for analysis.

To perform riboswitch positive selection, M9B minimal medium with 20 g/l glucose, 10 μg/ml vitamin B1, 200 μM Ni^{2+} and different amounts of NeuAc (4 g/l, 8 g/l, 12 g/l) was used. To perform riboswitch negative selection, M9B minimal medium with 20 g/l glucose, 10 μg/ml vitamin B1 and 10 μg/ml tetracycline was used. When cells reached to the late-exponential stage (OD_{600} = 1.0–1.2), the culture was transferred to fresh selection medium with 1% inoculum. Positive selection and negative selection were alternated for three rounds.

To perform pathway optimization, M9B minimal medium with 20 g/l glucose, 10 μg/ml vitamin B1, 200 μM Ni^{2+} was used. Single colonies were inoculated into each well of a 96-well plate, and green

fluorescence was detected using a Multi-Detection Microplate Reader.

To perform age_a selection, M9B minimal medium with 20 g/l glucose, 10 μg/ml vitamin B_1, 200 μM Ni^{2+} and 200 μM IPTG was used. When cells reached to the late-exponential stage, the culture was transferred to fresh selection medium with 1% inoculum. After three serial cultivations, negative selection was performed as described above.

To perform NeuAc batch fermentation, a single colony was inoculated into 5 ml LB medium containing the appropriate antibiotics and incubated for 12 h at 37 °C. The pre-culture was then inoculated into 50 ml of fresh MTB medium containing 20 g/l glucose and 200 μM IPTG with 4% inoculum. Fermentation was performed at 30 °C and 220 rpm, and pH was maintained at approximate 7.0 by 30% NH_4OH throughout the fermentation. Samples were taken at 6 h or 12 h (at night) intervals for analysis. The conditions and methods of fed-batch fermentation are the same as those of batch fermentation, but when the glucose is less than 10 g/l, the glucose is added to 20 g/l.

2.4. Analytical methods

Optical density (OD) was measured at 600 nm with a spectrophotometer (Shimazu, Japan). Fermentation samples were centrifuged at 12,000 rpm for 5 min and the supernatant was used for extracellular metabolites detection. Glucose, NeuAc, acetate, ethanol, formate, pyruvate, GlcNAc and ManNAc were quantitatively determined by HPLC (Shimadzu, Japan) equipped with a refractive index detector (RID-10A) (Shimadzu, Japan) and an Aminex HPX-87H ion exclusion column (Bio-Rad, USA) as described previously (Li et al., 2013). NeuAc levels were additionally determined by a resorcinol based colorimetric assay (Hooks et al., 2013).

3. Results and discussion

3.1. Designing a method for in vivo evolution of high threshold riboswitches

An *in vivo* NeuAc biosensor was constructed by placing the NeuAc aptamer upstream of *sfgfp* under the control of promoter P_{23106}, resulting plasmid pS-gfp, in our previous study (Yang et al., 2017), and the same construction without NeuAc riboswitch was named p-gfp. Although this biosensor was successfully constructed and responded to NeuAc in *vivo*, we did not spend much efforts on tuning its sensitivity and dynamic properties in previous paper, so we don't know if this aptazyme-based biosensor can work well for screening much higher NeuAc yield strain. In order to accurately characterize the properties of riboswitch *in vivo*, first of all, the exogenous NeuAc should not be diverted. Thus, *nanA*, the first gene of NeuAc degradation pathway was deleted from the genome of *E. coli* DH5α, resulting strain D5A. To characterize the designed NeuAc sensor *in vivo*, exogenous NeuAc ranging from 0 g/l to 8 g/l was added to D5A strains harboring plasmid pS-gfp and p-gfp, respectively, and the fluorescence intensity was measured. As shown in Fig. 1, the fluorescence intensity decreased in D5A/pS-gfp with increased exogenous NeuAc addition, while no obvious fluorescence alteration was observed in negative control. With 4 g/l NeuAc added, there was about a 5.8-fold decrease of the fluorescence. The fluorescence intensity at 8 g/l NeuAc was almost the same as that at 4 g/l NeuAc, indicating that 4 g/l NeuAc had already saturated the riboswitch and the threshold is quite low.

To improve the threshold, an *in vivo* riboswitch evolution method was developed to screening riboswitch mutant library. NeuAc riboswitch comprise an aptamer and a hammerhead ribozyme (Cho et al., 2013). Two loops of the aptamer are NeuAc binding domain, which contains 18 nts and was adopted for random mutagenesis (Fig. S1). The dual selection marker *tetA* was adopted to screen high threshold riboswitches (Muranaka et al., 2009). In our strategy, positive screening is performed using Ni^{2+} to remove too high threshold or nonresponsive riboswitches, because these riboswitches had a less down-regulation of

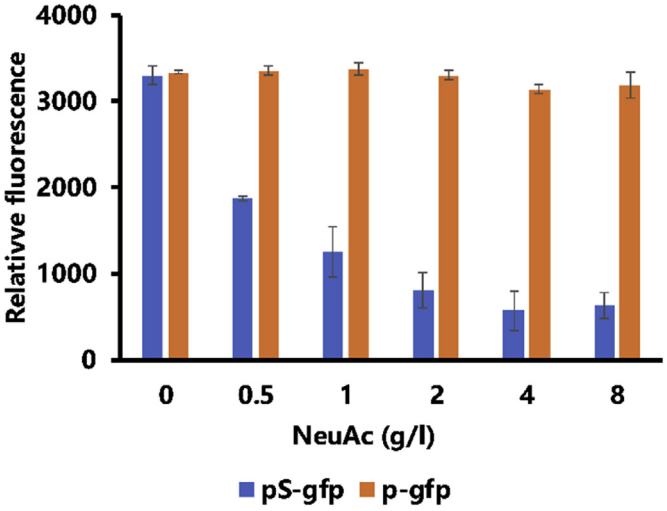

Fig. 1. Characterization of the NeuAc riboswitch and determination of selection conditions. (A) Using *sfgfp* as the reporter gene, effects of exogenously added NeuAc on the fluorescence intensity of D5A/p-gfp or D5A/pS-gfp were shown. Strains were cultured in M9B medium with 2% glucose. The fluorescence intensity of *sfgfp* was normalized by OD_{600}.

tetA at high concentration of NeuAc than the low threshold riboswitches, resulting slow growth on Ni^{2+}. And then negative screening is performed using tetracycline to remove low threshold riboswitches, because these riboswitches would more thoroughly turned off the expression of *tetA* when at low NeuAc concentration than those high threshold riboswitches, resulting incapable of growing on tetracycline (Fig. 2). One positive screening and one negative screening were defined as one round of screening. Then the positive and negative screening is performed in turn for three rounds to enrich the modified riboswitches. Finally, the riboswitch with threshold limited to the appropriate range should be enriched and screened out (Fig. S2).

3.2. Determination of riboswitch screening conditions

The gene *sfgfp* was fused to the c-terminal of *tetA* linked by a 3 GS linker for characterizing. To determinate selection conditions, different concentrations of Ni^{2+} or tetracycline were tried under given NeuAc concentrations. We found that the strain showed most obvious growth difference at 200 μM Ni^{2+} or 10 μg/ml tetracycline (Figs. S3 and S4). Using the measured conditions, significant growth differences were obtained in shake flask. The selection conditions were further demonstrated to be effective in shake flask (Fig. 3A and B). The fluorescence intensity proved that the expression level of *tetA* was negatively correlated with the concentration of NeuAc.

To demonstrate the feasibility of the screening method, an enrichment assay using defined model libraries was performed. Three strains, D5A/pTrc99a (no *tetA* expression), D5A/99a-tetA-gfp (constitutively expressed tetA) and D5A/99a-rs-tetA-gfp (tetA expression controlled by riboswitch), were co-cultured in M9B medium at a ratio of 1:1:1 and 100:100:1. After three rounds positive screening and negative screening alternately, the culture was subjected to single colony isolation. Colony PCR was performed to evaluate the proportion of three strains. For a total of 3 independent replicates of the experimental group at 1:1:1 ratio, the proportion of D5A/99a-rs-tetA-gfp was 96%, 96%, and 100%, respectively. For a total of 3 independent replicates of the experimental group at 100:100:1 ratio (Strain containing riboswitch was inoculated in smaller proportions), the proportion of D5A/99a-rs-tetA-gfp was 96%, 92%, and 100%, respectively (Fig. S5). This means a more than 184-fold enrichment of the strain D5A/99a-rs-tetA-gfp was obtained. This result demonstrated the feasibility of the designed selection method in riboswitch selection process.

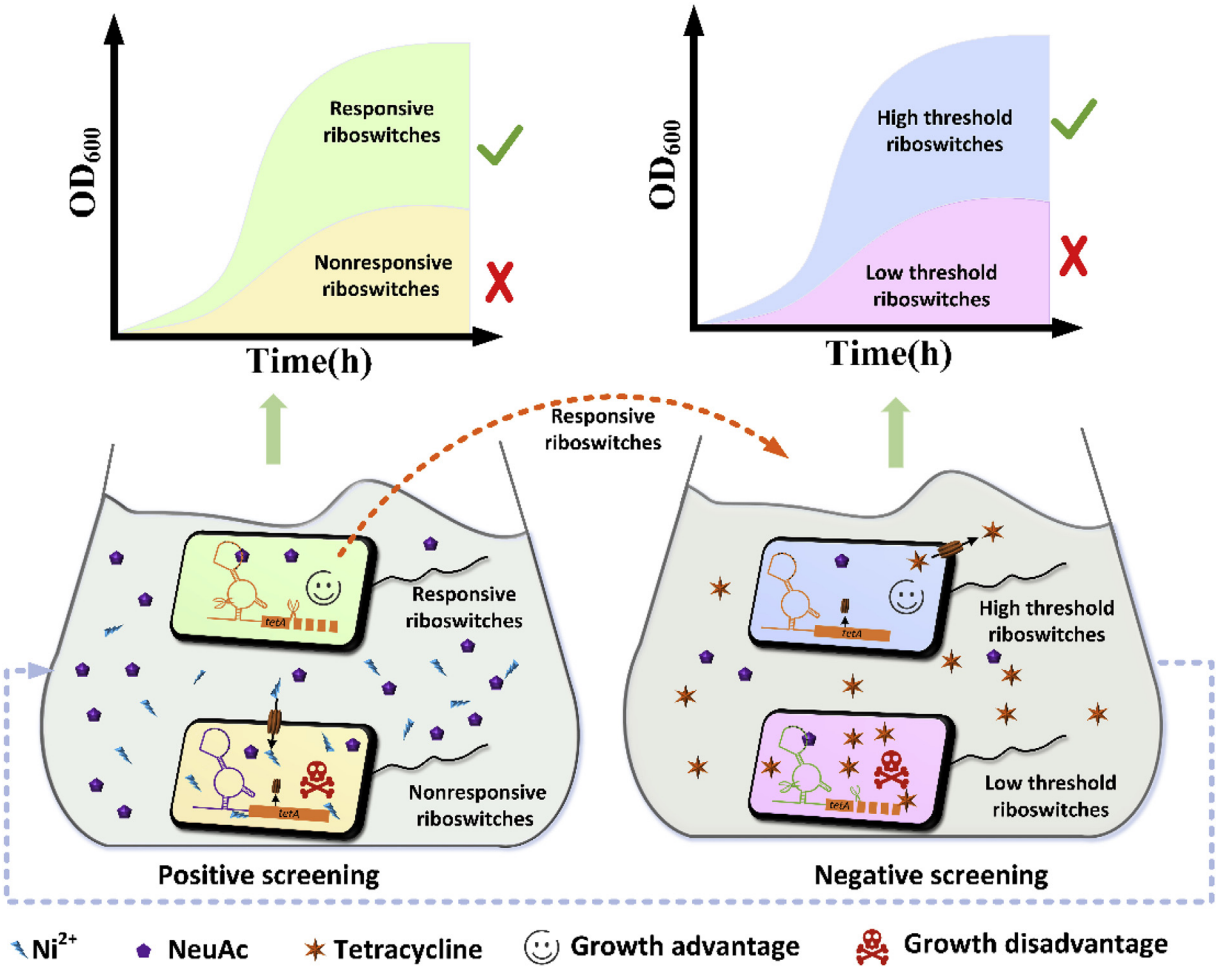

Fig. 2. In vivo evolution method of riboswitches. When high concentration of NeuAc is present, the normal riboswitches have self-cleavage activity, preventing *tetA* expression, thus the cells survive in the presence of Ni^{2+}. The unresponsive riboswitch normally expresses *tetA*, and the TetA protein imports Ni^{2+}, resulting in cell death. When there is low concentration of NeuAc, the normal riboswitch normally expresses *tetA*, the cells survive normally with tetracycline. The low threshold riboswitches have self-cleavage activity, and tetracycline kills cells. The curve at the bottom shows the growth of cells with different riboswitches in either positive or negative screening.

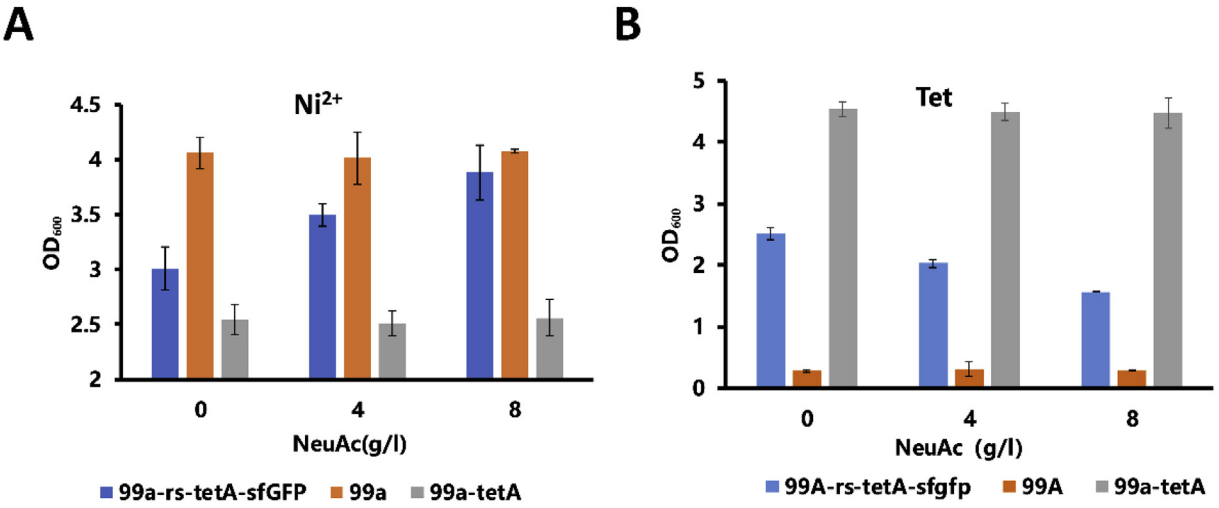

Fig. 3. Determination of selection conditions. (A) Ni^{2+} screening effect verification in shake flask. Using *tetA* as the reporter gene, effects of exogenously added NeuAc on intracellular NeuAc and cell growth of D5A/99a-rs-tetA-gfp, D5A/99a or D5A/99a-tetA were shown. Strains were cultured in M9B minimal medium with 2% glucose and 200 μM Ni^{2+}. Results are averages from three independent experiments, with standard deviations indicated by error bars. (B) Tetracycline screening effect verification in shake flask. Using *tetA* as the reporter gene, effects of exogenously added NeuAc on intracellular NeuAc and cell growth of D5A/99a-rs-tetA-gfp, D5A/99a or D5A/99a-tetA were shown. Strains were cultured in M9B minimal medium with 2% glucose and 10 μg/ml tetracycline.

Table 1
Characterization of riboswitch mutants.

Name	Mutants[a]	Enrichment percentage[b]	Threshold (g/l)	Sensitivity	Dynamic range
Rso	–	–	9.77	45.9	1.64
Rsa	A32G	50%	21.97	43.55	2.15
Rsb	T31C	83%	15.43	18.65	3.25
Rsc	T24C	42%	9.9	27.46	1.19
Rsd	C34T	42%	18.38	39.69	3.12

[a] For riboswitch selection, tree independent experiments were performed with 4 g/l, 8 g/l and 12 g/l NeuAc. Rsa was enriched in experiment group 1 with 4 g/l NeuAc in positive screening and 2 g/l NeuAc in negative screening. Rsb was enriched in experiment group 2 with 8 g/l NeuAc in positive screening and 4 g/l NeuAc in negative screening. Rsc and Rsd were enriched in experiment group 3 with 12 g/l NeuAc in positive screening and 8 g/l NeuAc in negative screening.

[b] The enrichment percentage was determined by the sum of one kind of plasmid dividing total sequenced clones. "-"indicates selection experiment was not performed.

3.3. In vivo evolution of NeuAc riboswitch with high threshold

To generate new NeuAc riboswitch with modified threshold, a library of riboswitch mutants was constructed. Single-base mutations were introduced into 18 nucleotides in the ligand-binding region of the NeuAc riboswitch using 18 designated primers, each with a degenerate base N (including A, T, C and G). Screening was conducted in three groups. Group 1 was screened with 4 g/l NeuAc in positive screening and 2 g/l NeuAc in negative screening. Group 2 was screened with 8 g/l NeuAc in positive screening and 4 g/l NeuAc in negative screening. Group 3 was screened with 12 g/l NeuAc in positive screening and 8 g/l NeuAc in negative screening. At each group, 24 randomly selected colonies were sequenced. In group one, Rsa was screened out 12 times, accounting for 50% and other mutants have been detected less than 1 time. At group two, Rsb was detected 20 times, and the rest mutants are all different. Rsc and Rsd were detected 10 times respectively from group three and the rest mutants are all different. Four riboswitch mutants were significantly enriched at rates of 50%, 83%, 42% and 42%, respectively (Table 1). Sequence information for riboswitch mutants is shown in Fig. S6.

The mutants enriched from the library were characterized using green fluorescent protein. Ligand response range of Rsa and Rsd expanded markedly (Fig. 4A). Taking Rsa as an example, its dose-response curve became slower decreased, but can keep falling in a large concentration range of NeuAc (0–35 g/l), while Rso only responded to a range of about 0–15 g/l NeuAc. The threshold, sensitivity and dynamic range were calculated according to the method (Mannan et al., 2017). The thresholds of the four mutants were 21.97 g/l, 15.43 g/l, 9.90 g/l and 18.38 g/l, respectively, which were significantly increased compared to the original riboswitch Rso (9.77 g/l) (Table 1). The sensitivity of Rsa and Rsd is basically the same as the original Rso, and is higher than Rsb and Rsc. The dynamic range of Rsb and Rsd is larger than Rso, Rsa and Rsc. Rsc has low threshold, low sensitivity and small dynamic range. Taken together, Rsd is the best mutant, because it has the high threshold, the high sensitivity and the large dynamic range. After deleting the *sfgfps* of four biosensors, the growth-coupled selection were characterized in M9B medium with 200 μM Ni^{2+} (Fig. 4B). Rsd exhibit largest growth changes at a wide range of NeuAc concentrations. Molecular docking and molecular dynamics simulations were performed to obtain the three-dimensional structure and ligand binding information of riboswitch mutants. Through structural align between Rsa and Rsd, minor structural changes were found (Figs. S6A, S6B, S6C). The calculated binding free energy showed that the mutants were more energetically favorable than the original riboswitch (Fig. S6D), which indicates that their substrate binding capacity/specificity were unaffected. The reason for the threshold change may be caused by coupling binding to an unfavorable binding-induced folding event. A theory was put forward that the distal mutation can alter riboswitches characteristics without altering specificity (Ricci et al., 2016), which was demonstrated by the kinetic simulations of riboswitch mutants. To detect the response effect of riboswitch biosensor at the population level, the fluorescence intensity distribution of riboswitches was determined by flow cytometry (Fig. S9), and results shown that fluorescence changes were uniform, which indicate that cells are responding in the same way.

3.4. Pathway optimization using the evolved NeuAc riboswitch

To prove the usefulness of the new generated riboswitch, the NeuAc biosynthesis pathway was again evolved and optimized according to

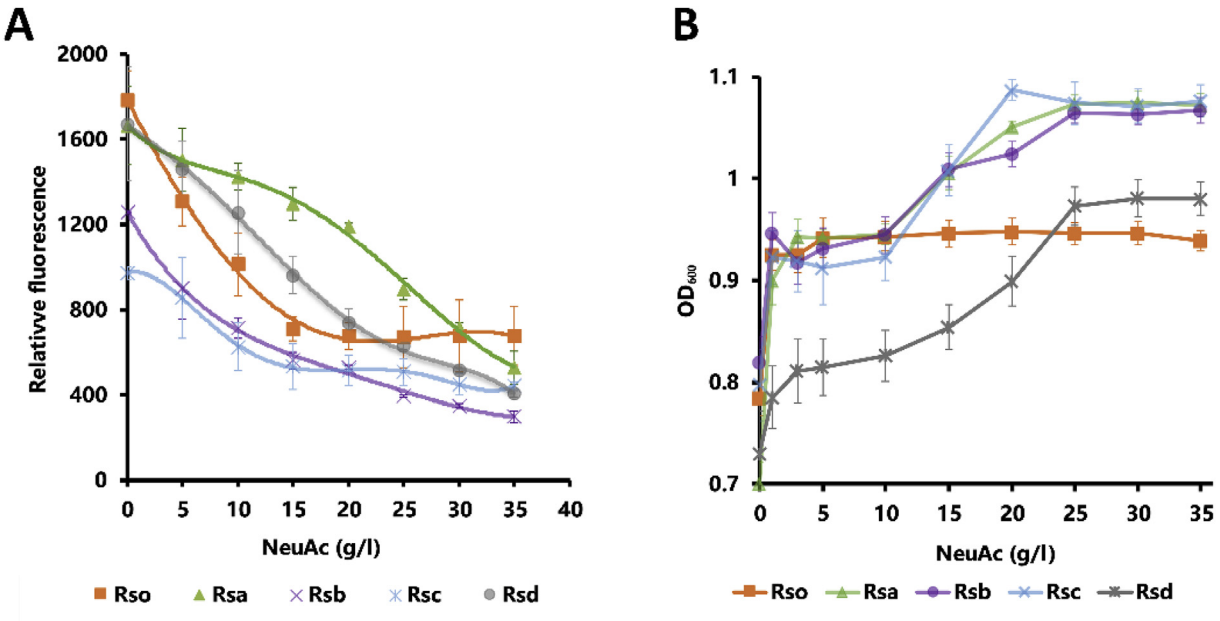

Fig. 4. Characterization of selected NeuAc riboswitch. (A) Comparison of the response curves of riboswitches. Relative fluorescence in the presence of NeuAc at various concentrations were fitted. (B) Comparison of the growth curve of riboswitches with different concentration NeuAc under Ni^{2+} screening.

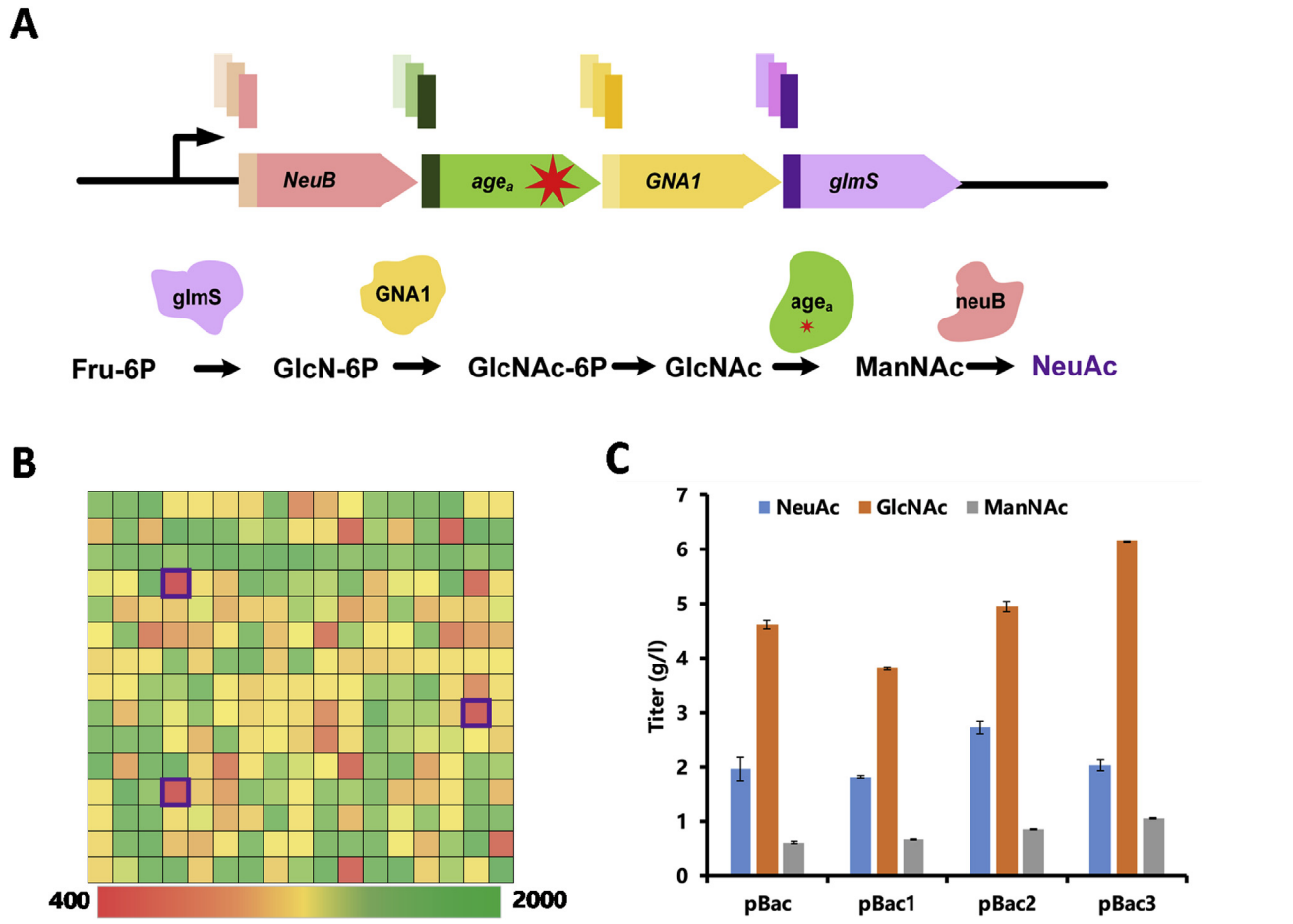

Fig. 5. Fluorescence of RBS selection and batch fermentation results. (A) Schematic presentation of NeuAc synthesis pathway in engineered *E. coli*. Genes: *glmS*, feedback resistant GlcN-6-P synthase; *GNA1*, GlcN-6-P N-acetyltransferase; age_a, GlcNAc 2-epimerase; $neuB_c$, NeuAc synthase. Abbreviations: Fru-6P, fructose-6-phosphate; GlcN-6P, glucosamine-6-phosphate; GlcNAc-6P, N-acetylglucosamine-6-phosphate; GlcNAc, N-acetylglucosamine; ManNAc, N-acetylmannosamine; NeuAc, N-acetylneuraminate. The red squares represent the RBS of the four genes, and a red star represents the presence of a mutation. (B) Fluorescence of 384 selected colonies. Red means low fluorescence, green means high fluorescence. The three lowest fluorescent squares are marked with purple boxes. (C) Batch-fermentation for NeuAc production in engineered *E. coli* strains. Blue indicates neuraminic acid, orange indicates acetylglucosamine, and gray indicates acetylmannosamine. (For interpretation of the references to color in this figure legend, the reader is referred to the Web version of this article.)

Table 2
Characterization of age_a mutants.

Name	NeuB mutants[a]	Enrichment percentage[b]
A	T910G	17%
B	T1108G	54%
C	A1058C	13%
D	G98C	43%

[a] For age_a evolution, two independent experiments were performed. A and B were enriched in experiment group 1. C and D were enriched in experiment group 2.

[b] The enrichment percentage was determined by the sum of one kind of plasmid dividing total sequenced clones.

the method we developed previously. The NeuAc biosynthesis pathway was constructed by overexpressing a feedback resistant GlcN-6-P synthase from *E. coli* MG1655 (*glmS**), a GlcN-6-P N-acetyltransferase from *Saccharomyces cerevisiae* EBY100 (*GNA1*), a GlcNAc 2-epimerase from *Anabaena* sp. CH1 (age_a), and a NeuAc synthase from *Campylobacter jejuni* ($neuB_c$) (Fig. 5A). The resulting plasmid was named pBac. To optimize this pathway, we engineered the RBS of the above four enzymes. The same strong RBS (AAGGAGATATACC) was initially used for all genes. Fine-tuning of this pathway was done via RBS engineering. The three groups of RBS were used to form mutant library by changing RBSs of the four genes using mixed primers in plasmid pBac, followed by Gibson assembly as described previously (Yang et al., 2017) (Table S4).

To test the effectiveness of new modified riboswitch, the riboswitch Rsd were cloned into a p15A-ori plasmid to generate p15A-Sdg. The mutant library was transformed into DN5 harboring p15A-Sdg. Then, 384 single colonies were inoculated into four 96-well plates for green fluorescence detection (Fig. 5B). The three RBS combinations with the lowest fluorescence were selected (Table S5). DN5/pBac with three group RBS mutants were used for batch fermentation. As a result, DN5/pBac2 and DN5/pBac3 produced more NeuAc than the original strain DN5/pBac (Fig. 5C). DN5/pBac2 produced 2.73 g/l NeuAc at 36 h (~39% improved compared with DN5/pB), which is the highest yield among tested strains. Glucose consumption rates and growth of the three strains were comparable to that of DN5/pB, but the accumulation of GlcNAc, ManNAc and NeuAc increased (Fig. 5C).

3.5. Evolution of key enzyme age using the evolved NeuAc riboswitch

In many studies, *slr1975* from *Synechocystis* sp. PCC 6803 was used to catalyze GlcNAc into ManNAc. This reversible enzyme uses ATP as activator and is inhibited by excess pyruvate. It has a relatively low affinity for ATP, which limited the catalytic efficiency (Zhang et al., 2010). In this study, acylglucosamine 2-epimerase (age_a) from

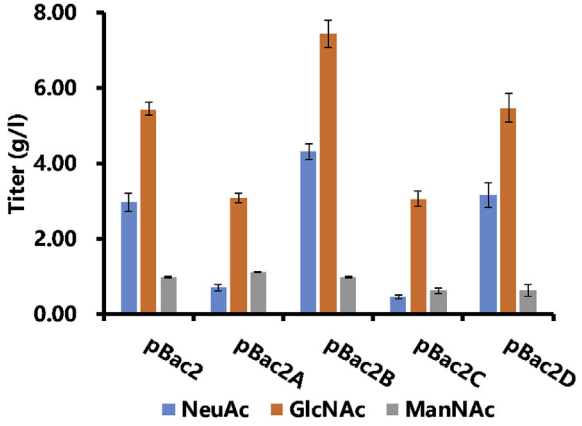

Fig. 6. Batch fermentation result of engineered strains with different *age* mutants at 36 h. A single colony was inoculated into 5 ml LB medium containing the appropriate antibiotics and incubated for 12 h at 37 °C. The pre-culture was then inoculated into 50 ml of fresh MTB medium containing 20 g/l glucose and 200 μM IPTG with 4% inoculum. Fermentation was performed at 30 °C and 220 rpm, and pH was maintained at approximate 7.0 by 30% NH_4OH throughout the fermentation. Samples were taken at 6 h or 12 h intervals for analysis. Fermentation was stopped at 36 h.

Anabaena sp. CH1 was used to replace *slr1975*, which has a relatively high affinity for ATP. However, accumulation of GlcNAc indicates a bottleneck still exist in GlcNAc epimerization (Fig. 5B). We thus chose N-acylglucosamine 2-epimerase (age_a) to increase its activity using riboswitch with high threshold. The mutagenetic age_a gene generated by error-prone PCR was used to replace the wild type age_a on pBac. The mutant library was transformed into DN5 and then evolved and screened using the new NeuAc riboswitch.

The evolution process was stopped after three rounds and 24 randomly selected colonies were sequenced and four variants were enriched (Table 2). Variants B and D reached to 54% and 42% of the total population, respectively. Two other mutants, A and C were also enriched, although in a lesser extent. The four best age_a mutants were cloned into pBac2 (replacing the wild type age_a) to evaluate the NeuAc production. Both B and D produced more NeuAc than the wild type age_a. DN5/pBac2B produced 4.32 g/l NeuAc (45% improved than DN5/pBac2), and DN5/pBac2D produced 3.16 g/l (7% improved than DN5/pBac2) (Fig. 6).

To evaluate the NeuAc production potential of DN5/pBac2B, we performed fed-batch fermentation in shake flasks. As shown in Fig. 7A, DN5/pBac2B produced 14.23 g/l NeuAc after 120 h. Only small quantity of ManNAc, formate, acetate and ethanol were detected, but still considerable amounts GlcNAc was accumulated (Fig. 7B). GlcNAc accumulation was due to the characteristic of *age*. *age* is a reversible enzyme which uses ATP as activator. New age_a may have higher conversion specific activity and we obtained a higher ratio of ManNAc and GlcNAc in the medium. In previous experiments, we used the original riboswitch to increase the production of NeuAc, while the production of NeuAc was only increased by 6% (Yang et al., 2017). The threshold of the riboswitch limited the further evolution of NeuAc biosynthesis. Using the new riboswitch, which have high threshold and large dynamic range, the key enzyme and RBS were further optimized and the production of NeuAc further increased by 42%.

4. Conclusion

As a flexible regulatory element, riboswitch has been widely used in metabolic engineering, but its properties often need improved and optimized. Here, we established an *in vivo* riboswitch evolution method and selected the modified riboswitch with a high threshold, a high sensitivity and a large dynamic range. As an example, we were able to improve the NeuAc production to14.32 g/l with new riboswitch facilitated RBS optimization and *age* evolution. This is the highest NeuAc titer that has been reported using glucose as the sole carbon source by fermentation. This screening method can be regarded as a generalized method for effectively improving the properties of other riboswitches.

CRediT authorship contribution statement

Qingxiao Pang: Data curation, Formal analysis, Investigation, Methodology, Writing - original draft. **Hao Han:** Data curation, Formal analysis. **Xiaoqin Liu:** Data curation, Formal analysis. **Zhiguo Wang:** Formal analysis, Methodology, Software, Visualization. **Quanfeng Liang:** Writing - review & editing. **Jin Hou:** Writing - review & editing. **Qingsheng Qi:** Conceptualization, Funding acquisition, Investigation, Project administration, Writing - review & editing. **Qian Wang:** Conceptualization, Funding acquisition, Investigation, Methodology, Project administration, Resources, Supervision, Validation,

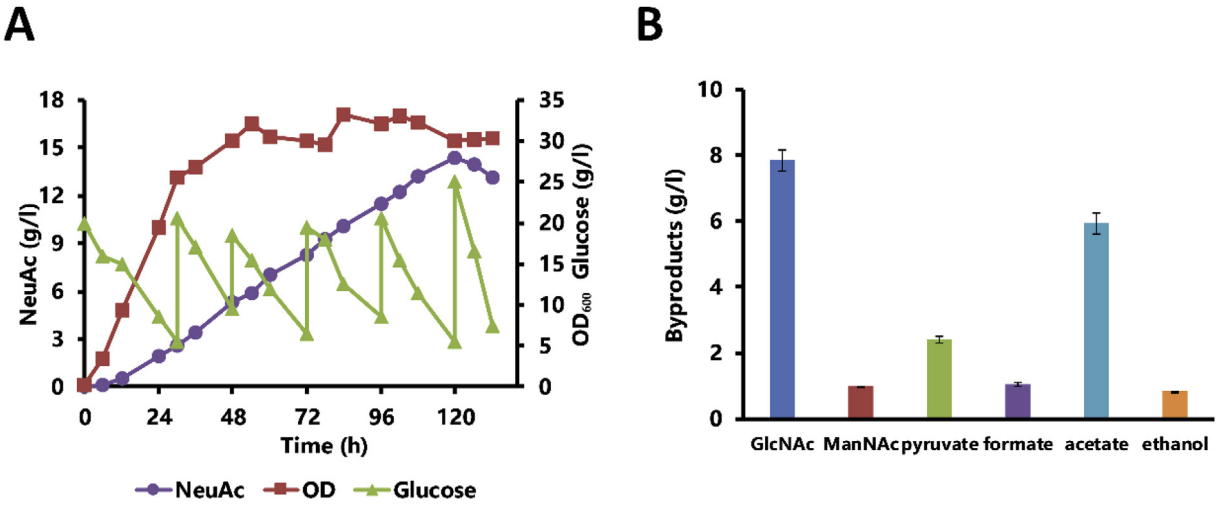

Fig. 7. Fermentation profile of DN5/pBac2B for NeuAc production. (A) A single colony was inoculated into 5 ml LB medium containing the appropriate antibiotics and incubated for 12 h at 37 °C. The pre-culture was then inoculated into 50 ml of fresh MTB medium containing 20 g/l glucose and 200 μM IPTG with 4% inoculum. Fermentation was performed at 30 °C and 220 rpm, and pH was maintained at approximate 7.0 by 30% NH_4OH throughout the fermentation. Samples were taken at 6 h or 12 h intervals for analysis. Fermentation was stopped at 132 h. For clarification, a representative curve from three independent experiments was shown, with standard differences (RSD) less than 10%. (B) Byproducts formation of DN5/pBac2B after 120 h fermentation.

Visualization, Writing - review & editing.

Declaration of competing interest

The authors declare no competing financial interests.

Acknowledgements

This work was financially supported by grants from the National Natural Science Foundation of China (31670077, 31730003) and Young Scholars Program of Shandong University.

Appendix A. Supplementary data

Supplementary data to this article can be found online at https://doi.org/10.1016/j.ymben.2020.01.002.

References

Aghdam, E.M., Hejazi, M.S., Barzegar, A., 2016. Riboswitches: from living biosensors to novel targets of antibiotics. Gene 592, 244–259.
Auslander, S., Ketzer, P., Hartig, J.S., 2010. A ligand-dependent hammerhead ribozyme switch for controlling mammalian gene expression. Mol. Biosyst. 6, 807–814.
Barrick, J.E., 2009. Predicting riboswitch regulation on a genomic scale. In: Serganov, A. (Ed.), Riboswitches: Methods and Protocols. Humana Press, Totowa, NJ, pp. 1–13.
Barrick, J.E., Corbino, K.A., Winkler, W.C., Nahvi, A., Mandal, M., Collins, J., Lee, M., Roth, A., Sudarsan, N., Jona, I., Wickiser, J.K., Breaker, R.R., 2004. New RNA motifs suggest an expanded scope for riboswitches in bacterial genetic control. Proc. Natl. Acad. Sci. U. S. A. 101, 6421–6426.
Breaker, R.R., 2011. Prospects for riboswitch discovery and analysis. Mol. Cell 43, 867–879.
Carothers, J.M., Goler, J.A., Keasling, J.D., 2009. Chemical synthesis using synthetic biology. Curr. Opin. Biotechnol. 20, 498–503.
Cho, S., Lee, B.R., Cho, B.K., Kim, J.H., Kim, B.G., 2013. In vitro selection of sialic acid specific RNA aptamer and its application to the rapid sensing of sialic acid modified sugars. Biotechnol. Bioeng. 110, 905–913.
Corbino, K.A., Barrick, J.E., Lim, J., Welz, R., Tucker, B.J., Puskarz, I., Mandal, M., Rudnick, N.D., Breaker, R.R., 2005. Evidence for a second class of S-adenosylmethionine riboswitches and other regulatory RNA motifs in alpha-proteobacteria. Genome Biol. 6, R70.
de la Pena, M., Garcia-Robles, I., Cervera, A., 2017. The hammerhead ribozyme: a long history for a short RNA. Molecules 22, 78.
Dietrich, J.A., McKee, A.E., Keasling, J.D., 2010. High-throughput metabolic engineering: advances in small-molecule screening and selection. Annu. Rev. Biochem. 79 (79), 563–590.
Ellington, A.D., Szostak, J.W., 1990. In vitro selection of RNA molecules that bind specific ligands. Nature 346, 818–822.
Felletti, M., Hartig, J.S., 2017. Ligand-dependent Ribozymes. Wires Rna page e1395.
Findeiss, S., Etzel, M., Will, S., Morl, M., Stadler, P.F., 2017. Design of artificial riboswitches as biosensors. Sensors 17 (9).
Gebetsberger, J., Micura, R., 2017. Unwinding the twister ribozyme: from structure to mechanism. RNA 8 (3), e1402.
Gibson, D.G., 2011. Enzymatic assembly of overlapping DNA fragments. Synth. Biol. 498, 349–361.
Gibson, D.G., Young, L., Chuang, R.Y., Venter, J.C., Hutchison, C.A., Smith, H.O., 2009. Enzymatic assembly of DNA molecules up to several hundred kilobases. Nat. Methods 6 343-U41.
Henkin, T.M., 2008. Riboswitch RNAs: using RNA to sense cellular metabolism. Genes Dev. 22, 3383–3390.
Hooks, D.O., Blatchford, P.A., Rehm, B.H.A., 2013. Bioengineering of bacterial polymer inclusions catalyzing the synthesis of N-acetylneuraminic acid. Appl. Environ. Microbiol. 79, 3116–3121.
Jang, S., Jang, S., Xiu, Y., Kang, T.J., Lee, S.H., Koffas, M.A.G., Jung, G.Y., 2017. Development of artificial riboswitches for monitoring of naringenin in vivo. ACS Synth. Biol. 6, 2077–2085.
Lee, S.W., Oh, M.K., 2015. A synthetic suicide riboswitch for the high-throughput screening of metabolite production in Saccharomyces cerevisiae. Metab. Eng. 28, 143–150.
Li, Y.K., Li, M.J., Zhang, X., Yang, P., Liang, Q.F., Qi, Q.S., 2013. A novel whole-phase succinate fermentation strategy with high volumetric productivity in engineered Escherichia coli. Bioresour. Technol. 149, 333–340.
Liu, C.C., Arkin, A.P., 2010. The case for RNA. Science 330, 1185–1186.
Mannan, A.A., Liu, D., Zhang, F.Z., Oyarzun, D.A., 2017. Fundamental design principles for transcription-factor-based metabolite biosensors. ACS Synth. Biol. 6, 1851–1859.
Mayer, G., Famulok, M., 2006. High-throughput-compatible assay for glmS riboswitch metabolite dependence. Chembiochem 7, 602–604.
McCown, P.J., Corbino, K.A., Stav, S., Sherlock, M.E., Breaker, R.R., 2017. Riboswitch diversity and distribution. RNA 23, 995–1011.
Muranaka, N., Sharma, V., Nomura, Y., Yokobayashi, Y., 2009. An efficient platform for genetic selection and screening of gene switches in Escherichia coli. Nucleic Acids Res. e39.
Nudler, E., Mironov, A.S., 2004. The riboswitch control of bacterial metabolism. Trends Biochem. Sci. 29, 11–17.
Ogawa, A., 2011. Rational design of artificial riboswitches based on ligand-dependent modulation of internal ribosome entry in wheat germ extract and their applications as label-free biosensors. RNA 17, 478–488.
Pavlova, N., Kaloudas, D., Penchovsky, R., 2019. Riboswitch distribution, structure, and function in bacteria. Gene 708, 38–48.
Penchovsky, R., Stoilova, C.C., 2013. Riboswitch-based antibacterial drug discovery using high-throughput screening methods. Expert Opin. Drug Discov. 8, 65–82.
Ricci, F., Vallée-Bélisle, A., Simon, A.J., Porchetta, A., Plaxco, K.W., 2016. Using nature's "tricks" to rationally tune the binding properties of biomolecular receptors. Accounts Chem. Res. 49, 1884–1892.
Rogers, J.K., Taylor, N.D., Church, G.M., 2016. Biosensor-based engineering of biosynthetic pathways. Curr. Opin. Biotechnol. 42, 84–91.
Roth, A., Breaker, R.R., 2009. The structural and functional diversity of metabolite-binding riboswitches. Annu. Rev. Biochem. 78, 305–334.
Serganov, A., Huang, L., Patel, D.J., 2008. Structural insights into amino acid binding and gene control by a lysine riboswitch. Nature 455, 1263–1267.
Serganov, A., Nudler, E., 2013. A decade of riboswitches. Cell 152, 17–24.
Sherwood, A.V., Henkin, T.M., 2016. Riboswitch-mediated gene regulation: novel RNA architectures dictate gene expression responses. Annu. Rev. Microbiol. 70, 361–374.
Souliere, M.F., Altman, R.B., Schwarz, V., Haller, A., Blanchard, S.C., Micura, R., 2013. Tuning a riboswitch response through structural extension of a pseudoknot. Proc. Natl. Acad. Sci. U.S.A. 110, E3256–E3264.
Wang, J.M., Gao, D.F., Yu, X.L., Li, W., Qi, Q.S., 2015. Evolution of a chimeric aspartate kinase for L-lysine production using a synthetic RNA device. Appl. Microbiol. Biotechnol. 99, 8527–8536.
Williams, T.C., Pretorius, I.S., Paulsen, I.T., 2016. Synthetic evolution of metabolic productivity using biosensors. Trends Biotechnol. 34, 371–381.
Winkler, W.C., Breaker, R.R., 2005. Regulation of bacterial gene expression by riboswitches. Annu. Rev. Microbiol. 59, 487–517.
Winkler, W.C., Nahvi, A., Roth, A., Collins, J.A., Breaker, R.R., 2004. Control of gene expression by a natural metabolite-responsive ribozyme. Nature 428, 281–286.
Xiao, Y., Bowen, C.H., Liu, D., Zhang, F.Z., 2016. Exploiting nongenetic cell-to-cell variation for enhanced biosynthesis. Nat. Chem. Biol. 12, 339.
Yang, P., Wang, J., Pang, Q., Zhang, F., Wang, J., Wang, Q., Qi, Q., 2017. Pathway optimization and key enzyme evolution of N-acetylneuraminate biosynthesis using an in vivo aptazyme-based biosensor. Metab. Eng. 43, 21–28.
Zhang, J., Jensen, M.K., Keasling, J.D., 2015. Development of biosensors and their application in metabolic engineering. Curr. Opin. Chem. Biol. 28, 1–8.
Zhang, Y.N., Tao, F., Du, M.F., Ma, C.Q., Qiu, J.H., Gu, L.C., He, X.F., Xu, P., 2010. An efficient method for N-acetyl-d-neuraminic acid production using coupled bacterial cells with a safe temperature-induced system. Appl. Microbiol. Biotechnol. 86, 481–489.
Zhou, L.B., Zeng, A.P., 2015. Engineering a lysine-ON riboswitch for metabolic control of lysine production in corynebacterium glutamicum. ACS Synth. Biol. 4, 1335–1340.